International Journal of
Molecular Sciences

MDPI

Article

Analytical Investigations and Molecular Dynamics Simulations of 3-Miktoarm Star (3-Arm μ-Star) Copolymers A_2B and AB_2

Pawel Karbowniczek and Zoriana Danel *

Faculty of Materials Engineering and Physics, Cracow University of Technology, 30-719 Cracow, Poland
* Correspondence: zoriana.danel@pk.edu.pl

Abstract

The analytical investigations of 3-miktoarm star (3-arm μ-star) copolymers of type A_2B and AB_2 are performed in the framework of mean-field approximation and Flory–Huggins theory. The total entropy of mixing and the Helmholtz free energy of interaction are calculated for the number N_A monomers of type A and number N_B monomers of type B, respectively. The results confirm that the Helmholtz free energy of miktoarm star copolymers differs from that of polymer blends. The temperature dependence of the Helmholtz free energy allowed us to construct a phase diagram of the solution of miktoarm star copolymers, showing regions of stability, instability, and metastability. The analytical results confirm that a miktoarm star copolymer is not merely a mixture of different homo-arm star polymers and are consistent with a previous investigation performed by liquid chromatography under the critical conditions. Moreover, we performed molecular dynamics simulations of a dilute solution of 3-miktoarm star copolymer of type A_2B with a certain number of beads (300 + 300 + 200 + 1) and star copolymer of type AB_2 with number of beads (300 + 200 + 200 + 1), accordingly. The calculations of the radius of gyration and monomer density profiles of the 3-miktoarm star copolymers of type A_2B and AB_2 in confined geometry of two repulsive surfaces (Dirichlet–Dirichlet boundary conditions) and one repulsive and other one attractive surface (Dirichlet–Neumann boundary conditions) by molecular dynamics simulations are performed. The obtained analytical and numerical results indicate that a dilute solution of miktoarm star copolymers can be used in biotechnology and medicine for drug and gene transmission as well as for the production of new functional materials.

Keywords: critical phenomena; polymers; molecular dynamics simulations; surface effects

Academic Editor: Haiyang Gao

Received: 21 April 2026
Revised: 21 May 2026
Accepted: 27 May 2026
Published: 2 June 2026

1. Introduction

The investigation of star polymers, which are a simple example of branched macromolecules with at least three linear chains radiating from a central core, attracts the attention of scientists from both academic and practical points of view due to their unique properties, such as a low viscosity, a high functional group density, and specific core–shell architecture, which enabled several potential applications as thermoplastic elastomers and drug carriers in materials engineering, nanoscience, biology, and medicine (see [1,2] and references therein).

Depending on the chemical compositions of the arms, star polymers can be classified into two categories: (1) star homopolymers, which consist of a symmetrical structure comprising radiating arms with identical chemical composition and similar molecular weight or (2) mikto-arm (or heteroarm) star copolymers, which contain two or more

arms with different chemical compositions and can have different molecular weights and different peripheral functionality. As it is known [3], there are several approaches that can be employed for the synthesis of star copolymers: the "core-first" approach, the "arm-first" synthesis, a combination of the "arm-first" and "core-first" approaches, and "grafting onto" a functionalized core via "click" chemistry.

In 1963, Orofino and Wenger [4] used tri(chloromethyl) benzene in combination with anionic polymerization as a linking agent for the first time in order to prepare 3-arm star homopolystyrenes. Some time later, Pennisi and Fetters [5] reported the synthesis of 3-arm asymmetric star homopolymers of homopolystyrenes and polybutadienes. It should be mentioned that, for the first time, synthesis of a 3-arm μ-star copolymer consisting of two polyisoprene and one homopolystyrene arm was presented in [6]. Moreover, in 1992, the synthesis of a 3-arm μ-star terpolymer of homopolystyrenes, polyisoprenes, and polybutadiene was published in [7]. Later in a series of papers [8–16], different 3-arm miktoarm star polymers were synthesized by anionic polymerization and selective chlorosilane-based linking chemistry, respectively.

The results of the investigation performed by liquid chromatography under the critical conditions [17] delivered the final proof that a miktoarm star copolymer containing two or more compositionally different arms connected to a single molecule arises. Thus, it was finally confirmed that a miktoarm star copolymer arises, and it is not just a mixture of different homo-arm star polymers.

It should be mentioned that miktoarm star copolymers are a relatively new and unique class of macromolecules, which are interesting due to their intriguing properties that can be tailored by modification of their polymer arms and have found wide applications in medicine, biology, materials engineering, nanotechnology, and nanolithography. There are many papers devoted to these subjects, and below we list some of them. For example, miktoarm star (μ-star) polymers have been extensively investigated in a series of studies as carriers for drug encapsulation [18,19] and anticancer drug delivery applications [20–27] due to their excellent biocompatibility, cell staining performance, and rapid redox responsiveness. Miktoarm star copolymers of type A_2B and AB_2 can easily self-assemble into soft nanoparticles [19]. One of the most common examples of such soft nanoparticles is spherical micelles. Miktoarm star polymers enable the introduction of a different arrangement of hydrophobic/hydrophilic components inside of such micelles. It has been demonstrated that the core–shell structures formed from miktoarm star copolymers upon microphase separation in water yield spherical assemblies with smaller hydrodynamic diameters in comparison to their linear analogs with similar molecular weights and demonstrate higher drug loading efficiencies [22,23].

Moreover, μ-star polymers display exceptional antimicrobial possibilities originating from their tunable biological properties and can be used as antimicrobial agents in order to combat the most common hospital-acquired pathogens and multidrug-resistant Gram-negative bacteria with high therapeutic indices and good selectivity toward pathogens over mammalian cells [28]. It should be mentioned that in the case of using μ-star copolymers as antimicrobial agents, no resistance to bacteria A. baumannii was observed. The extraordinary antimicrobial effectiveness of μ-star polymers was possible due to a multimodal mechanism of bacterial cell death by outer membrane destabilization with the unregulated movement of ions across the cytoplasmic membrane and the induction of the apoptotic-like cell death pathway [28]. Moreover, in [29], an excellent antimicrobial effectiveness of miktoarm star polymers composed of polylysine and glycopolymer toward Gram-positive bacteria was reported.

Miktoarm star polymers can self-assemble into novel and complex morphologies that are inaccessible via the self-assembly of conventional block copolymers. For exam-

ple, the research presented in [30] was devoted to the fabrication of nanostructured thin films through self-assembly, which has attracted considerable attention as a method for economical generation of the patterns with higher resolution than optical lithography. It should be mentioned that the molecular configuration and structural ordering of miktoarm star polymers in thin films can differ significantly from those in bulk. The reason for such a difference is related to the architectural effects of miktoarm star polymers under confinement, coupled with interfacial interactions at the substrate and surface. Many unique self-assembly phenomena arise when the star structure becomes highly asymmetric, for example, having one A arm and multiple B arms, as is in the case of miktoarm star copolymers of type A_2B and AB_2. This type of arm asymmetry induces significant phase boundary deflection compared to linear polymers due to conformational effects [31,32].

Recently, the influence of solvent quality and substrate-block interactions in thin films of A_2B_2 miktoarm star polymers was investigated by coarse-grained molecular dynamics simulations with a bead-spring model [33]. The results of investigation obtained in [33] indicate that μ-star polymers require a longer time to form a well-ordered cylinder structure than a lamellae structure. In addition, in [33], it was mentioned that, compared to linear block copolymers, μ-star polymers are characterized by much slower self-assembly kinetics with smaller domains. Thus, further investigation of μ-star polymers under confinement is essential to understanding their self-assembly behavior.

The present paper is devoted to an analytical and numerical investigation of the simplest form of 3-arm μ-star copolymers of type A_2B and AB_2 in infinite space and under confinement of two parallel walls with different boundary conditions. Taking into account the mean-field approach and the Flory–Huggins theory, we performed the calculation of the total entropy of mixing and the Helmholtz free energy of mixing for simplified lattice model of 3-arm μ-star copolymers of type A_2B and AB_2 and determine the regions of stability, instability, and metastability of the mixed state for the above-mentioned dilute solution of miktoarm star copolymers. Such an investigation is important because it enables us to obtain the phase diagram of miktoarm star copolymers. Moreover, taking into account the bead–spring model, we performed molecular dynamic calculations of the monomer density profiles for a dilute solutions of 3-arm μ-star copolymers of type A_2B and AB_2 in confined geometries like a slit of two parallel walls with different boundary conditions.

2. Results and Discussion

2.1. Analytical Results for 3-Miktoarm Star (3-Arm μ-Star) Copolymers A_2B and AB_2

The results of calculations for the Helmholtz free energy $\Delta F'_{mix}(\phi, T)/k_B$ for the 3-arm μ-star copolymer of type A_2B as a function of the volume fraction $\phi'_A = \phi$ at $\phi_C = 0.0012$ and $\phi_C = 0.0014$ for star copolymer AB_2 for temperatures T = 300 K, 325 K, 350 K, 375 K are presented in Figure 1. In Figure 2, we present, for comparison, the results for the Helmholtz free energy of polymer blends with the number N_A monomers of type A and number N_B monomers of type B according to the results analyzed in [34].

As it is possible to see from Figure 1, the results for the 3-arm μ-star copolymer of type A_2B with number $N_A = 300$ monomers of type A and number $N_B = 200$ monomers of type B are different from the results for polymer blends on Figure 2, with the respective number of monomers of type A and B.

The results finally confirm that the Helmholtz free energy of 3-miktoarm star copolymers differs from the results for the Helmholtz free energy of polymer blends, as shown in Figures 1 and 2. Thus the obtained analytical results confirm that a 3-miktoarm star copolymer it is not just a mixture of different homo-arm star polymers and are in agreement with the investigation performed using liquid chromatography under the critical conditions [17] as mentioned above.

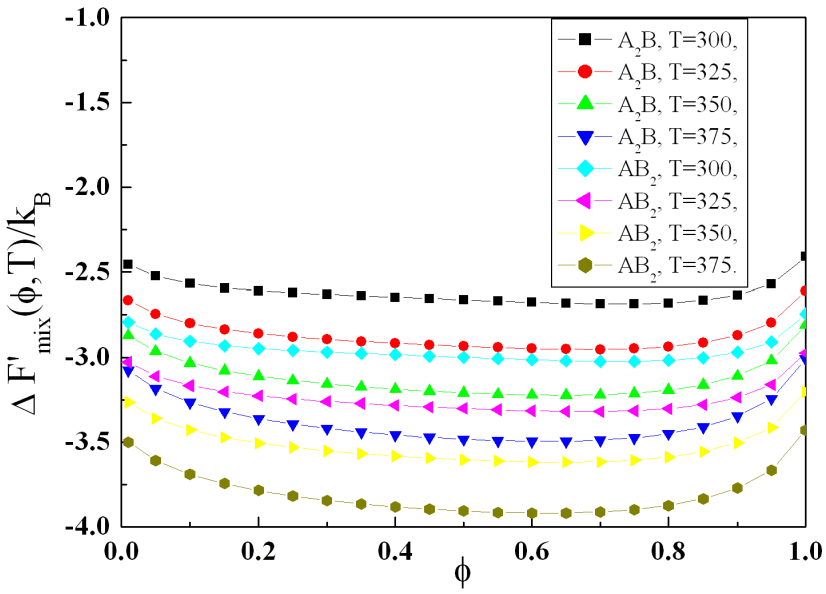

Figure 1. The Helmholtz free energy for hypothetical 3-miktoarm star copolymer A_2B as function of ϕ at $\phi_C = 0.0012$ and for star copolymer AB_2 as a function of ϕ at $\phi_C = 0.0014$ for temperatures T = 300 K, 325 K, 350 K, 375 K with the Flory interaction parameters χ_1 = (2.5 K)/T, χ_2 = (3 K)/T, χ_3 = (3.5 K)/T.

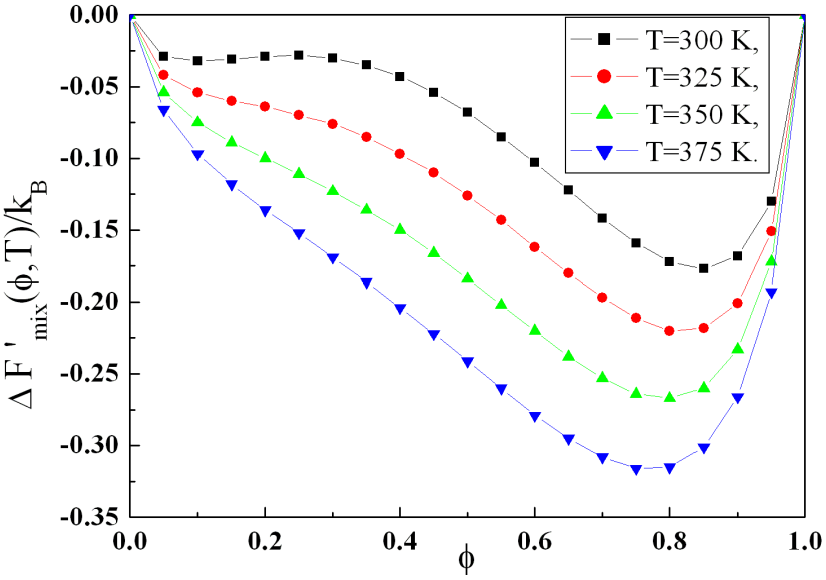

Figure 2. The Helmholtz free energy for hypothetical polymer blends as a function of ϕ at temperatures T = 300 K, 325 K, 350 K, 375 K with the Flory interaction parameter χ = (2.5 K)/T obtained according to [34,35].

The dependence of binodal $\chi_{1,b}$ (see Equation (17) from composition ϕ for μ-star copolymers A_2B and AB_2 is presented on Figure 3. It should be mentioned that the binodal coincides with the coexistence curve.

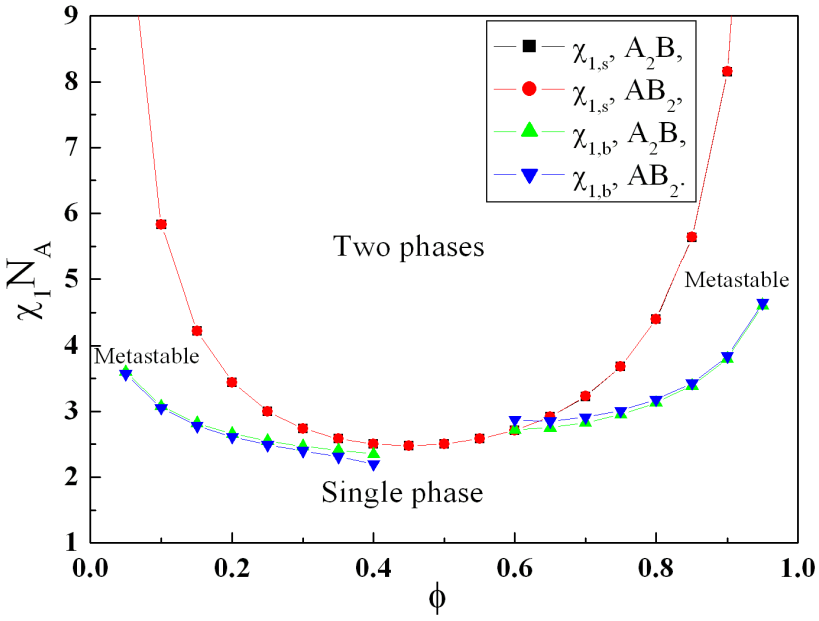

Figure 3. Phase diagram of μ-star copolymers A_2B at $\phi_C = 0.0012$ and AB_2 at $\phi_C = 0.0014$. The dependence of $\chi_1 N_A$ from composition ϕ.

For the second derivative of the Helmholtz free energy (see Equation(15)) of 3-arm μ-star copolymer, we obtain

$$\frac{\partial^2 \Delta F'_{mix}}{\partial \phi^2} = k_B T\left(\frac{1}{N_A \phi} + \frac{1}{N_B(1-\phi-\phi_C)} - 2\chi_1\right). \quad (1)$$

It should be mentioned that the second derivative of the Helmholtz free energy (see Equation (1)) of 3-arm μ-star copolymers A_2B with $\phi_C = 0.0012$ and AB_2 with $\phi_C = 0.0014$ is positive in the whole region of composition $0 \leq \phi \leq 1$. The inflection points in $\Delta F'_{mix}(\phi, T)$ can be found by equating the second derivative of the free energy to zero: $\frac{\partial^2 \Delta F'_{mix}}{\partial \phi^2} = 0$. The curve corresponding to the inflection point is the boundary between unstable and metastable regions and is named the spinodal, which in our case is

$$\chi_{1,s} = \frac{1}{2}\left(\frac{1}{N_A \phi} + \frac{1}{N_B(1-\phi-\phi_c)}\right). \quad (2)$$

The lowest point on the spinodal curve corresponds to the critical point and can be obtained by equating the first derivative of the spinodal to zero

$$\frac{\partial \chi_{1,s}}{\partial \phi} = \frac{1}{2}\left(-\frac{1}{N_A \phi^2} + \frac{1}{N_B(1-\phi-\phi_C)^2}\right) = 0. \quad (3)$$

The solving of Equation (3) gives us the critical composition

$$\phi_{cr} = \frac{(1-\phi_C)\sqrt{N_B}}{\sqrt{N_A} + \sqrt{N_B}}. \quad (4)$$

After substituting Equation (4) into Equation (2), we can obtain critical interaction parameter $\chi_{1,cr} \approx 2.4777$ for μ-star copolymer A_2B and $\chi_{1,cr} \approx 2.4782$ for μ-star copolymer AB_2. The dependence of the spinodal $\chi_{1,s}$ from composition ϕ is presented in Figure 3.

The spinodal and binodal curves meet at the critical point, as shown in Figure 3. For interaction parameter $\chi_1 < \chi_{1,cr}$ the homogeneoas mixture is stable at any composition. For the case $\chi_1 > \chi_{1,cr}$ there is a miscibility gap between the two branches of the binodal. It

should be mentioned that for any composition within a miscibility gap, the equilibrium state consists of two phases. The points on the phase diagram between the spinodal curve and binodal curve correspond to metastable mixtures (see Figure 3). As shown in Figure 3, the phase diagram for miktoarm star copolymers differs from that for polymer blends (see [34]).

2.2. Numerical Results for Monomer Density Profiles of 3-Arm μ-Star Copolymers A_2B and AB_2

To solve the equations of motion we used a program written in C++, that implements the Verlet integration scheme with a time step $\Delta t = 0.005$. Simulations were performed in the NVT ensemble; therefore, we used a thermostat with constant temperature $T = 1$ applied every selected number of time steps (200).

First, in order to determine the radius of gyration of the star polymer and its copolymer counterparts, we performed 20 simulations over 11×10^3 time steps (10^3 for equilibration and 10^4 for data acquisition). We have obtained $R_g = 29.7(12)$ for homopolymer star with three arms, which is in agreement with our previous result $R_g = 30.69$ obtained in [36], and then we calculated the radius of gyration $R_g = 29.82(72)$ for 3-arm μ-star copolymer A_2B and $R_g = 29.33(98)$ for 3-arm μ-star copolymer AB_2. Therefore, as seen from these results, there are no statistically significant differences in the radius of gyration of copolymers with the same length of arms. Then, we performed simulations with different boundary conditions: two repulsive (Dirichlet–Dirichlet) and repulsive–attractive (Dirichlet–Neumann) walls. In both cases, we analyzed the situations where the distance between walls is equal to $2R_g$ and $R_g/2$. In order to present the results, we normalized the distance between the walls to 1 and each density profile to $\int_0^1 \rho(z)dz = \frac{R_g}{L}$.

Exemplary configurations of star polymer with three arms and copolymers between two walls with separation $L = 2R_g$ for the Dirichlet–Dirichlet boundary conditions are presented in Figure 4. Monomer density profiles, presented in Figures 5 and 6, suggest that there is no difference between star homopolymers and copolymers A_2B and AB_2 for two repulsive walls in the case where we have the copolymers with the same length of arms. However, there is a significant difference in the adsorption of polymers for the case of one attractive wall, where copolymers adsorb better than the usual star-shaped polymers because of the stronger interaction with the wall. The difference is caused by the shape of the wall-particle potential. The repulsive part of the Lennard–Jones 9-3 potential is very strongly inclined, and therefore, the change in its effect for copolymers is almost imperceptible. However, for attractive interaction, the potential has a minimum that is greater for copolymers, and this causes an increased absorption to the wall.

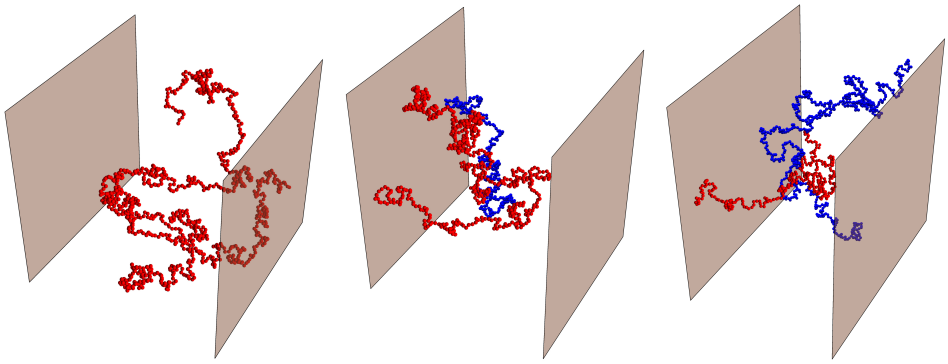

Figure 4. Exemplary configurations of star polymer with three arms and 3-arm μ-star copolymers A_2B and AB_2 for the case of two repulsive walls at the distance $L = 2R_g$. Red color of monomers corresponds to the normal arm with $\epsilon = 1$ and blue color to copolymer arms with $\epsilon = 4$.

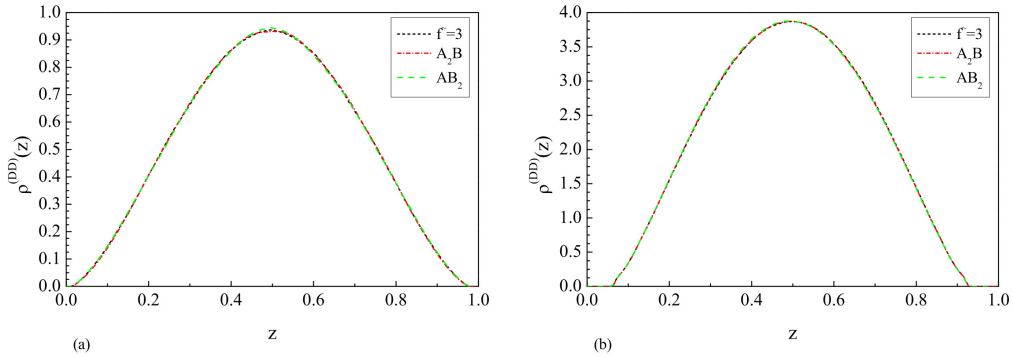

Figure 5. Monomer density profiles $\rho(z)$ of star-shaped polymer with three arms and 3-arm μ-star copolymers A_2B and AB_2 between two repulsive walls. The separation of the walls is equal to (**a**) $L = 2Rg$ and (**b**) $L = R_g/2$.

Moreover, we analyzed the influence of the lengths of μ-star copolymer arms on the adsorption properties. Arms interacting with the Lennard–Jones potential with parameter $\epsilon = 4$ were built of 200 monomers, giving a total number of 801 monomers $(300 + 300 + 200 + 1)$ for A_2B copolymer and 701 monomers $(300 + 200 + 200 + 1)$ for AB_2 copolymer. First, we have calculated $R_g = 27.62(78)$ for A_2B copolymer and $R_g = 25.21(62)$ for AB_2 copolymer. Then, we simulated the above mentioned copolymers in a slit with Dirichlet–Dirichlet and Dirichlet–Neumann boundary conditions. For such polymers, monomer density profiles are presented in Figures 7 and 8. Like in the previous case, there is a significant difference in polymer adsorption for the case of one attractive and one repulsive wall (see Figure 8). However, the reduced length of copolymer arms that interact with a stronger potential also caused the differences for two repulsive walls (see Figure 7). In such a case, copolymers A_2B and AB_2 are more localized in the center of a slit than a homopolymer star with $\tilde{f} = 3$.

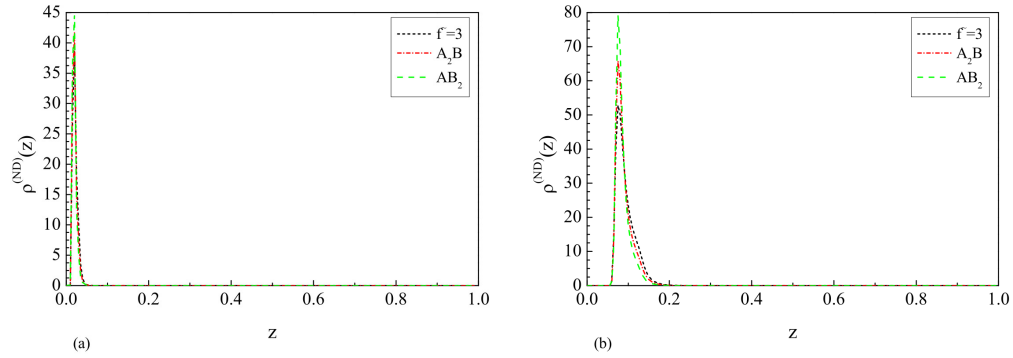

Figure 6. Monomer density profiles $\rho(z)$ of star-shaped polymer and 3-arm μ-star copolymers A_2B and AB_2 between one attractive and one repulsive wall. The separation of the walls is equal to (**a**) $L = 2Rg$ and (**b**) $L = R_g/2$.

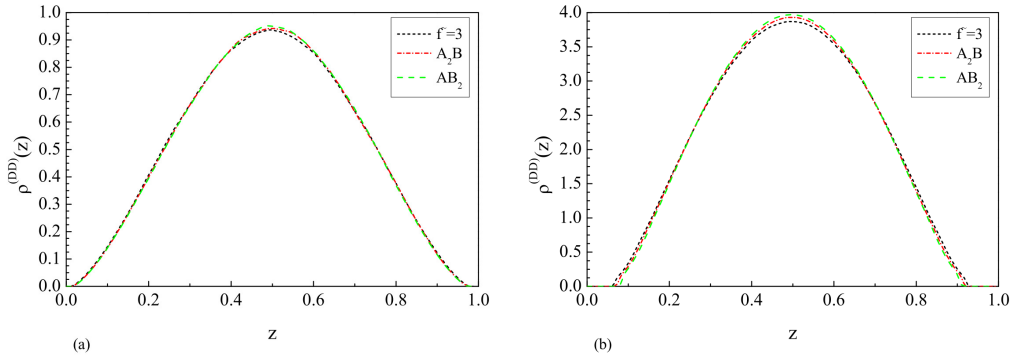

Figure 7. Monomer density profiles $\rho(z)$ of star-shaped polymer with 3 arms and 3-arm μ-star copolymers A_2B and AB_2 with different length of arms between two repulsive walls. The separation of the walls is equal to (**a**) $L = 2Rg$ and (**b**) $L = R_g/2$.

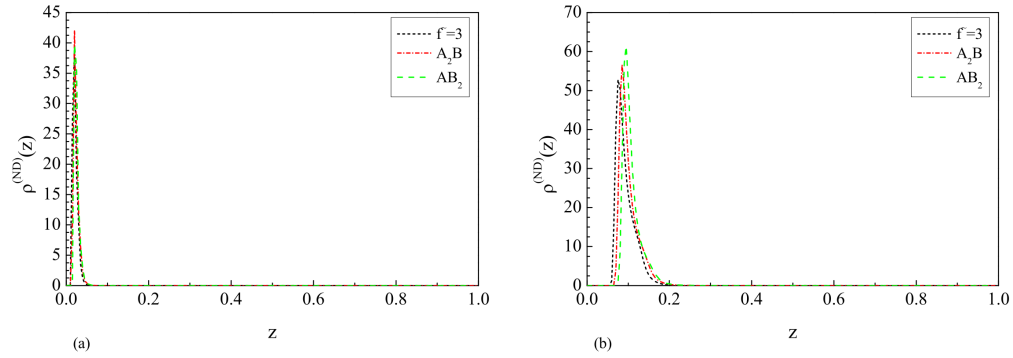

Figure 8. Monomer density profiles $\rho(z)$ of star-shaped polymer with 3 arms and 3-arm μ-star copolymers A_2B and AB_2 with different length of arms between one attractive and one repulsive wall. The separation of the walls is equal to (**a**) $L = 2Rg$ and (**b**) $L = R_g/2$.

3. Materials and Methods

3.1. Analytical Investigation of 3-Miktoarm Star (3-Arm μ-Star) Copolymers A_2B and AB_2

We apply a mean-field approach for the description of 3-arm μ-star copolymers of type A_2B, where we assume that we have two arms of type A and one arm of type B. Moreover, we performed an investigation of the μ-star copolymer of type AB_2, where we assumed that we have one arm of type A and two arms of type B. We assume that our copolymers can be modeled as a sequence of repeating units of two types, A and B, on the periodic lattice, and that the lattice sites are of the order of monomer sizes, but do not necessarily correspond exactly to the chemical monomers. We do not consider charged systems such as polyelectrolytes. The mean-field approach for polymer blends with two different macromolecular chains with length $N_A >> 1$ and $N_B >> 1$ [34] gives the possibility to calculate the total entropy of mixing per lattice site:

$$\Delta\tilde{S}_{mix} = \frac{\Delta S_{mix}}{n} = -k_B\left(\frac{\phi_A}{N_A} ln\phi_A + \frac{\phi_B}{N_B} ln\phi_B\right), \tag{5}$$

where ϕ_A and ϕ_B are the volume fraction of the two components in polymer blends:

$$\begin{aligned} \phi_A &= \frac{V_A}{V_A + V_B}, \\ \phi_B &= \frac{V_B}{V_A + V_B}, \end{aligned} \tag{6}$$

and $V_A = N_A\sigma$ is the molecular volume of a molecule of species A, $V_B = N_B\sigma$ is the molecular volume of a molecule of species B, and σ is the lattice site volume. It should be

mentioned that N_A and N_B are the numbers of lattice sites occupied by molecules of type A and type B, respectively. Taking into account the mean-field approach, we can obtain the total entropy of mixing per lattice site for the 3-arm μ-star copolymer:

$$\Delta\tilde{S}'_{mix} = \frac{\Delta S'_{mix}}{n'} = -k_B\left(\frac{\phi'_A}{N_A} ln\phi'_A + \frac{\phi'_B}{N_B} ln\phi'_B + \frac{\phi'_C}{N_C} ln\phi'_C\right), \quad (7)$$

where ϕ'_A, ϕ'_B, and ϕ'_C are the volume fraction of the A, B, C components in the 3-arm μ-star copolymer. For the case of a 3-arm μ-star copolymer with configuration A_2B, we have

$$\begin{aligned} \phi'_A &= \frac{2N_A}{2N_A + N_B + N_C}, \\ \phi'_B &= \frac{N_B}{2N_A + N_B + N_C}, \\ \phi'_C &= \frac{1}{2N_A + N_B + N_C}, \end{aligned} \quad (8)$$

where we assume that we have one monomer $N_C = 1$ of type C in the center of μ-star polymer. For the case of 3-arm μ-star copolymer AB_2, we have, respectively,

$$\begin{aligned} \phi'_A &= \frac{N_A}{N_A + 2N_B + N_C}, \\ \phi'_B &= \frac{2N_B}{N_A + 2N_B + N_C}, \\ \phi'_C &= \frac{1}{N_A + 2N_B + N_C}. \end{aligned} \quad (9)$$

We can perform calculations for the total entropy of mixing for 3-arm μ-star copolymer A_2B in the case where we have two arms of A type with $N_A = 300$ monomers and one arm of B type with $N_B = 200$ monomers, and one monomer in the center, which give us the total number of monomers: $N = 300 + 300 + 200 + 1$. We obtain obtain $\Delta\tilde{S}'_{mix} = 0.0105k_B$. It should be mentioned that, for polymer blends, in this case, we have $\Delta\tilde{S}_{mix} = 0.0025k_B$. The respective calculations for 3-arm μ-star copolymer of type AB_2 with $N = 300 + 200 + 200 + 1$ give us the following result: $\Delta\tilde{S}'_{mix} = 0.012k_B$. For polymer blends, in this case, we obtain $\Delta\tilde{S}_{mix} = 0.0028k_B$. As detailed, the mixing entropy is small for blends and μ-star copolymers, yet always positive, thereby promoting mixing. In addition, the mixing entropy for polymer blends is definitely smaller than the mixing entropy for μ-star polymers. The result in Equation (5) gives the possibility to obtain the free energy of mixing per site for polymer blends [34]:

$$\Delta\tilde{F}_{mix} = -T\Delta\tilde{S}_{mix} = k_BT\left(\frac{\phi_A}{N_A} ln\phi_A + \frac{\phi_B}{N_B} ln\phi_B\right). \quad (10)$$

By analogy, taking into account the result in Equation (7), we can calculate the free energy of mixing per site for 3-arm μ-star copolymers:

$$\Delta\tilde{F}'_{mix} = -T\Delta\tilde{S}'_{mix} = k_BT\left(\frac{\phi'_A}{N_A} ln\phi'_A + \frac{\phi'_B}{N_B} ln\phi'_B + \frac{\phi'_C}{N_C} ln\phi'_C\right). \quad (11)$$

In the general case, the free energy of mixing can be either negative, which promotes mixing, or positive, in which case mixing is opposed. To calculate the Helmholtz free energy of mixing, we can apply the Flory–Huggins theory [35], a simplified lattice model in which components are mixed at constant volume, including into calculations the energy of

interactions between components. Thus, as it was presented in [34,35], the energy change on mixing per lattice site for polymer blends is

$$\Delta\tilde{U}_{mix} = k_B T \chi \phi_A \phi_B, \tag{12}$$

where $\chi = \frac{z}{2}(\frac{2u_{AB}-u_{AA}-u_{BB}}{k_B T})$ is the Flory interaction parameter for polymer blends, z is the number of nearest neighbors and $z = 4$ for a square lattice, and $z = 6$ for a cubic lattice. The average pairwise interaction of a monomer of type A with one of its neighboring monomers is just a volume fraction weighted sum of interaction energies between monomers: $U_A = \phi_A u_{AA} + \phi_B u_{AB}$. For the monomer of type B the average pairwise interaction with one of its neighbors is $U_B = \phi_A u_{AB} + \phi_B u_{BB}$. Taking into account the Flory–Huggins theory [35], for the energy change per lattice site of 3-arm μ-star copolymer we obtain

$$\Delta\tilde{U}'_{mix} = k_B T(\chi_1 \phi(1-\phi-\phi_c) + \chi_2 \phi_c(1-\phi-\phi_c) + \chi_3 \phi\phi_C), \tag{13}$$

where we introduced the following interaction parameters χ_1, χ_2, χ_3:

$$\begin{aligned} \chi_1 &= \frac{z}{2}(\frac{2u_{AB}-u_{AA}-u_{BB}}{k_B T}), \\ \chi_2 &= \frac{z}{2}(\frac{2u_{BC}-u_{BB}}{k_B T}), \\ \chi_3 &= \frac{z}{2}(\frac{2u_{AC}-u_{AA}}{k_B T}). \end{aligned} \tag{14}$$

Here we took into account that, in the case of 3-miktoarm star copolymers, the average pairwise interaction of a monomer of type A with one of its neighboring monomers is $U'_A = \phi'_A u_{AA} + \phi'_B u_{AB} + \phi'_C u_{AC}$. For the monomer of type B in the case of 3-arm μ-star copolymers, the average pairwise interaction with one of its neighbors is $U'_B = \phi'_A u_{AB} + \phi'_B u_{BB} + \phi'_C u_{BC}$, and for the central monomer of type C, we have $U'_C = \phi'_A u_{AC} + \phi'_B u_{BC}$. Taking into account the above result in Equation (13), we can obtain the result for the Helmholtz free energy of mixing per lattice cite for the 3-arm μ-star copolymer:

$$\begin{aligned} \Delta F'_{mix} = \Delta\tilde{U}'_{mix} - T\Delta\tilde{S}'_{mix} &= k_B T(\frac{\phi}{N_A} ln\phi + \frac{(1-\phi-\phi_C)}{N_B} ln(1-\phi-\phi_C) + \\ + \frac{\phi_C}{N_C} ln\phi_C + \chi_1 \phi(1-\phi-\phi_C) &+ \chi_2 \phi_C(1-\phi-\phi_C) + \chi_3 \phi\phi_C), \end{aligned} \tag{15}$$

where we introduced the following notations: $\phi'_A = \phi$, $\phi'_B = 1-\phi'_A-\phi'_C = 1-\phi-\phi_C$, and $\phi'_C = \phi_C$. As it is possible to see from Equation (15), the first three terms in this equation have entropic origin, and in accordance with it, they always promote mixing. The last three terms in Equation (15) have energetic origin and can be positive, zero or negative depending on the sign of the respective interaction parameters χ_1, χ_2, χ_3.

One of the major assumptions of the Flory–Huggins theory is that there is no volume change during mixing, and the monomers of both species can fit on the lattice sites of the same lattice. As is known, in most real polymer blends, the volume per monomer changes after mixing. Additionally, some monomers may pack together better with certain other monomers. In the general case, all deviations from the lattice model are collected into the interaction parameters χ_1, χ_2 and χ_3, which display non-trivial dependences on composition, temperature, and chain length. We can assume that in the case of 3-arm μ-star copolymers the temperature dependences of the interaction parameters can be written as the sum of two terms: $\chi_1 = \alpha_1 + \beta_1/T$, $\chi_2 = \alpha_2 + \beta_2/T$ and $\chi_3 = \alpha_3 + \beta_3/T$, where α_i is "entropic part" and β_i/T with $i = 1,2,3$ is "entalpic part" of interaction parameters. The

temperature dependence of the Helmholtz free energy (see Equation (11)) allows us to construct a phase diagram that summarizes the phase behavior of solutions of miktoarm star polymers, showing regions of stability, instability, and metastability. In order to obtain the interaction parameter corresponding to the phase boundary, which is named binodal, we need to calculate the first derivative of the Helmoltz free energy with respect to composition and solve the following Equation

$$\frac{\partial \Delta F'_{mix}}{\partial \phi} = 0. \tag{16}$$

Taking into account the result for the Helmholtz free energy in Equation (15) and solving Equation (16) for the binodal, we obtain

$$\chi_{1,b} = \frac{1}{(2\phi + \phi_C - 1)}\left(\frac{1}{N_A} - \frac{1}{N_B} + \frac{\ln \phi}{N_A} - \frac{\ln(1-\phi-\phi_C)}{N_B} - \phi_C\chi_2 + \phi_C\chi_3\right). \tag{17}$$

The local stability of such a solution of miktoarm star polymers is determined by the sign of the second derivative of the Helmholtz free energy (see Equation (11)) with respect to composition ϕ

$$\begin{aligned} \frac{\partial^2 \Delta F'_{mix}}{\partial \phi^2} &< 0, -unstable, \\ \frac{\partial^2 \Delta F'_{mix}}{\partial \phi^2} &> 0, -locally \quad stable. \end{aligned} \tag{18}$$

3.2. Molecular Dynamics Simulations of 3-Arm μ-Star Copolymers A_2B and AB_2

To confirm our theoretical results, we performed molecular dynamics simulations of star-shaped copolymers with 3 arms. At the beginning, we investigated the case where polymers were built from 1 central monomer plus 3 arms, each consisting of 300 monomers, for a total number of 901 monomers.

The interaction between neighboring monomers in the polymer chain was modeled using FENE (finite extensible nonlinear elastic potential) [37]:

$$U_{FENE}(r) = \begin{cases} -\frac{1}{2}kR_0^2 \ln\left[1 - \left(\frac{r}{R_0}\right)^2\right] & \text{if } r < R_0, \\ +\infty & \text{if } r \geq R_0, \end{cases} \tag{19}$$

where we assumed $k = 30$ and $R_0 = 3/2$ and the WCA (Weeks–Chandler–Andersen) potential [38]:

$$U_{WCA}(r) = \begin{cases} -\epsilon & \text{if } r < 2^{1/6}\sigma, \\ 4\epsilon\left[\left(\frac{\sigma}{r}\right)^{12} - \left(\frac{\sigma}{r}\right)^{6}\right] & \text{if } r \geq 2^{1/6}\sigma. \end{cases} \tag{20}$$

Monomers, which were not neighbors, interacted via the 12-6 Lennard Jones potential [39]:

$$U_{12-6}(r) = 4\epsilon\left[\left(\frac{\sigma}{r}\right)^{12} - \left(\frac{\sigma}{r}\right)^{6}\right]. \tag{21}$$

The interaction with the walls was given by the 9-3 Lennard–Jones potential [40]:

$$U_{9-3}(r) = \frac{3\sqrt{3}}{2}\epsilon\left[\left(\frac{\sigma}{r}\right)^{9} - \left(\frac{\sigma}{r}\right)^{3}\right]. \tag{22}$$

This potential was used with a cut-off, which determined the type of polymer–wall interaction. For $R_{cut-off} = 3^{1/6}$, the wall was repulsive, and for $R_{cut-off} = 10$ attractive.

For the standard star-shaped polymer, we assumed $\epsilon = 1$ and $\sigma = 1$. However, in order to construct 3-arm μ-star copolymer, at least one arm has to interact differently. We assumed that the monomers of such arms have to interact with the greater strength represented by the different depth of the potential $\epsilon = 4$. We also assumed that all monomers have the same size $\sigma = 1$. By applying this, we also had to modify interactions with other arms and walls. In this case, we used well established Lorentz–Berthelot mixing rules [41,42] for the monomer radii

$$\sigma_{ij} = \frac{\sigma_{ii} + \sigma_{jj}}{2} \tag{23}$$

and diameters

$$\epsilon_{ij} = \sqrt{\epsilon_{ii}\epsilon_{jj}} \tag{24}$$

for the potential depth.

4. Conclusions

The analytical investigation of 3-miktoarm star (3-arm μ-star) copolymers of type A_2B and AB_2 is performed in the framework of the mean-field approach and Flory–Huggins theory. The total entropy of mixing and the Helmholtz free energy of interaction of 3-miktoarm star copolymers were calculated. The obtained results confirm that the Helmholtz free energy and phase diagram for miktoarm star copolymers differ from those for polymer blends, as shown in Figure 1, Figure 2, Figure 3, respectively. That means that a solution of miktoarm star copolymers is not just a mixture of different homo-arm star polymers, and this result is in agreement with previous investigation performed using liquid chromatography under the critical conditions. Our investigations allow us to determine the regions of stability, instability, and metastability for a dilute solutions of miktoarm star copolymers of type A_2B and AB_2. Moreover, we performed the calculation of the monomer density profiles of 3-miktoarm star copolymers of type A_2B and AB_2 in confined geometry of two repulsive surfaces, which corresponds to Dirichlet–Dirichlet boundary conditions and one repulsive and other one attractive surface, which corresponds to Dirichlet–Neumann boundary conditions by molecular dynamics simulations. We analyzed the influence of the lengths of μ-star copolymer arms on the adsorption properties. Arms interacting with the Lennard–Jones potential with parameter $\epsilon = 4$ were built of 200 monomers, and for the arms with 300 monomers, we assumed $\epsilon = 1$, giving a total amount of 801 monomers $(300 + 300 + 200 + 1)$ for A_2B copolymer and 701 monomers $(300 + 200 + 200 + 1)$ for AB_2 copolymer, respectively.

We obtained that the radius of gyration for μ-star copolymer A_2B is equal to $R_g = 27.62(78)$ and for μ-star copolymer AB_2 is $R_g = 25.21(62)$. These results are smaller than the result for the radius of gyration for a star homopolymer with three arms, which is $R_g = 29.7(12)$. We determined that there is a significant difference in polymer adsorption for the case of one attractive and other one repulsive wall in the case of 3-miktoarm star copolymers A_2B and AB_2, as shown in Figure 8. However, we found that the reduced length of copolymer arms interacting with a stronger potential also caused differences for two repulsive walls, as shown in Figure 7. The results indicate that in this case, 3-miktoarm star copolymers A_2B and AB_2 are more localized in the center of a slit than a homopolymer star with $\tilde{f} = 3$.

Miktoarm star copolymers of type A_2B and AB_2 have been widely used in medicine for drug delivery [43–46]. As mentioned above, miktoarm star copolymers of type A_2B and AB_2 can easily self-assemble into soft nanoparticles (or micelles) [19] and offer the possibility to introduce a different arrangement of hydrophobic/hydrophilic components inside of micelles. A series of papers [22,23] have demonstrated that the core–shell structures

formed from miktoarm star copolymers upon microphase separation in water yield spherical assemblies with smaller hydrodynamic diameters in comparison to their linear analogs with similar molecular weights, and in accordance with this, demonstrate higher drug loading efficiencies. Our obtained numerical results indicate that the radius of gyration for miktoarm star copolymers of type A_2B and AB_2 is smaller than the radius of gyration for homopolymer star [36] with three legs and the radius of gyration for linear polymer chain [47] with the same number of monomers. This result suggests that such miktoarm star copolymers can achieve higher drug-loading efficiencies than linear polymers and homopolymer stars.

Molecular dynamics simulations suggest that the monomer density profiles for 3-arm μ-star copolymers A_2B and AB_2 are bigger near the adsorbing wall than the respective monomer density for a homopolymer star with three arms, as it is possible to see from Figures 6 and 8. This causes a larger number of monomers in the miktoarm star copolymer to be situated near the adsorbing wall, thereby imposing a greater pressure on the wall than in homopolymer star solutions. This assumes a reduction in static friction in such materials, enabling using them for production of new types of MEMS and NEMS. Thus, the obtained analytical and numerical results indicate that a dilute solution of 3-miktoarm star copolymers can find practical application in biotechnology and medicine for drug and gene transmission, as well as for the production of new functional materials.

Author Contributions: Conceptualization, Z.D.; methodology, Z.D. and P.K.; software, P.K. and Z.D.; validation, P.K. and Z.D.; formal analysis, Z.D. and P.K.; investigation, P.K. and Z.D.; resources, Z.D. and P.K.; data curation, Z.D. and P.K.; writing—original draft preparation, Z.D. and P.K.; writing—review and editing, Z.D. and P.K.; visualization, P.K. and Z.D.; supervision, Z.D.; project administration, Z.D.; funding acquisition, Z.D. All authors have read and agreed to the published version of the manuscript.

Funding: This research received no external funding.

Institutional Review Board Statement: Not applicable.

Informed Consent Statement: Not applicable.

Data Availability Statement: The original contributions presented in this study are included in the article.

Conflicts of Interest: The authors declare no conflicts of interest.

References

1. Ren, J.M.; McKenzie, T.G.; Fu, Q.; Wong, E.H.H.; Xu, J.; An, Z.; Shanmugam, S.; Davis, T.P.; Boyer, C.; Qiao, G.G. Star Polymers. *Chem. Rev.* **2016**, *116*, 6743–6836. [CrossRef]
2. Wu, W.; Wang, W.; Li, J. Star Polymers: Advances in Biomedical Applications. *Prog. Polym. Sci.* **2015**, *46*, 55–85. [CrossRef]
3. Liu, M.; Blankenship, J.R.; Levi, A.E.; Fu, Q.; Hudson, Z.M.; Bates, C.M. Miktoarm Star Polymers: Synthesis and Applications. *Chem. Mater.* **2022**, *34*, 6188–6209. [CrossRef]
4. Orofino, T.A.; Wenger, F. Dilute solution properties of branched polymers. Polysterene trifunctional star molecules. *J. Phys. Chem.* **1963**, *67*, 566. [CrossRef]
5. Pennisi, R.W.; Fetters, L.J. Preparation of asymmetric 3-arm polybutadiene and polystyrene stars. *Macromolecules* **1988**, *21*, 1094. [CrossRef]
6. Mays, J.W. Synthesis of "simple graft" poly(isoprene-g-styrene) by anionic polymerization. *Polym. Bull.* **1990**, *23*, 247. [CrossRef]
7. Iatrou, H.; Hadjichristidis, N. Synthesis of a model 3-miktoarm star terpolymer. *Macromolecules* **1992**, *25*, 4649. [CrossRef]
8. Iatrou, H.; Siakali-Kioulafa, E.; Hadjichristidis, N.; Roovers, J.; Mays, J. Hydrodynamic properties of model 3-miktoarm star copolymers. *J. Polym. Sci. Part B Polym. Phys.* **1995**, *33*, 1925. [CrossRef]
9. Pitsikalis M.; Hadjichristidis, N. Model mono-, di-, and tri-, omega.-functionalized three-arm star polybutadienes. Synthesis and association in dilute solutions by membrane osmometry and static light scattering. *Macromolecules* **1995**, *28*, 3904. [CrossRef]

10. Tselikas, Y.; Iatrou, H.; Hadjichristidis, N.; Liang, K.S.; Mohanty, K.; Lohse, D.J. Morphology of miktoarm star block copolymers of styrene and isoprene. *J. Chem. Phys.* **1996**, *105*, 2456. [CrossRef]
11. Zioga, A.; Sioula, S.; Hadjichristidis, N. Synthesis and solution properties of star–shaped poly (tert-butyl acrylate). *Macromol. Symp.* **2000**, *157*, 239. [CrossRef]
12. Bellas, V.; Iatrou, H.; Hadjichristidis, N. Controlled anionic polymerization of hexamethylcyclotrisiloxane. Model linear and miktoarm star co- and terpolymers of dimethylsiloxane with styrene and isoprene. *Macromolecules* **2000**, *33*, 6993. [CrossRef]
13. Tsoukatos, T.; Hadjichristidis, N. Synthesis of model polycyclohexylene/polyethylene miktoarm star copolymers with three and four arms. *J. Polym. Sci. Part A Polym. Chem.* **2002**, *40*, 2575. [CrossRef]
14. Mavroudis, A.; Avgeropoulos, A.; Hadjichristidis, N.; Thomas, E.L.; Lohse, D.J. Synthesis and morphological behavior of model linear and miktoarm star copolymers of 2-methyl-1,3-pentadiene and styrene. *Chem. Mater.* **2003**, *15*, 1976. [CrossRef]
15. Fragouli, P.G.; Iatrou, H.; Hadjichristidis, N.; Sakura, T.; Hirao, A.Synthesis and characterization of model 3-miktoarm star copolymers of poly (dimethylsiloxane) and poly(2-vinylpyridine). *J. Polym. Sci. Part A Polym. Chem.* **2006**, *44*, 614. [CrossRef]
16. Krkensgaard, J.J.K.; Fragouli, P.; Hadjichristidis, N.; Mortensen, K. Perforated lamellae morphology in novel P2VP (PDMS-b-PI-b-PS)2 3-miktoarm star quarterpolymer. *Macromolecules* **2011**, *44*, 575. [CrossRef]
17. Gao, H.; Matyjaszewski, K. Synthesis of Low-Polydispersity Miktoarm Star Copolymers via A Simple "Arm-First" Method: Macromonomers as Arm Precursors. *Macromolecules* **2008**, *41*, 4250–4257. [CrossRef]
18. Aghajanzadeh, M.; Zamani, M.; Rostamizadeh, K.; Sharafi, A.; Danafar, H. The Role of Miktoarm Star Copolymers in Drug Delivery Systems. *J. Macromol. Sci. Part A* **2018**, *55*, 559–571. [CrossRef]
19. Lotocki, V.; Kakkar, A. Miktoarm Star Polymers: Branched Architectures in Drug Delivery. *Pharmaceutics* **2020**, *12*, 827. [CrossRef]
20. Wei, H.; Zhang, X.; Cheng, C.; Cheng, S.-X.; Zhuo, R.-X. Self-Assembled, Thermosensitive Micelles of A Star Block Copolymer Based on PMMA and PNIPAAm for Controlled Drug Delivery. *Biomaterials* **2007**, *28*, 99–107. [CrossRef]
21. Lin, W.; Nie, S.; Zhong, Q.; Yang, Y.; Cai, C.; Wang, J.; Zhang, L. Amphiphilic Miktoarm Star Copolymer (PCL)3-(PDEAEMA-b-PPEGMA)3 as pH-Sensitive Mecelles in the Delivery of Anticancer Drug. *J. Mater. Chem. B* **2014**, *2*, 4008–4020. [CrossRef]
22. Wang, M.; Zhang, X.; Peng, H.; Zhang, M.; Zhang, X.; Liu, Z.; Ma, L.; Wei, H. Optimization of Amphiphilic Miktoarm Star Copolymers for Anticancer Drug Delivery. *ACS Biomater. Sci. Eng.* **2018**, *4*, 2903–2910. [CrossRef]
23. Xiao, J.; He, Q.; Yang, M.; Li, H.; Qiu, X.; Wang, B.; Zhang, B.; Bu, W. Hierarchical self-assembly of miktoarm star copolymers with pathway complexity. *Polym. Chem.* **2021**, *12*, 1476–1486. [CrossRef]
24. Beach, M.A.; Nayanathara, U.; Gao, Y.; Zhang, C.; Xiong, Y.; Wang, Y.; Such, G.K. Polymeric nanoparticles for drug delivery. *Chem. Rev.* **2024**, *124*, 5505–5616. [CrossRef]
25. Kakkar, A. Miktoarm polymers: Past, present and future. *Nanomedicine* **2025**, *20*, 2193–2195. [CrossRef]
26. Baghbanbashi, M.; Kakkar, A. Polymersomes: Soft nanoparticles from miktoarm stars for applications in drug delivery. *Mol. Pharm.* **2022**, *19*, 1687–1703. [CrossRef]
27. Chen, C.; Guo, X.; Du, J.; Choi, B.; Tang, H.; Feng, A.; Thang, S.H. Synthesis of Multifunctional Miktoarm Star Polymers via An RGD Peptide-Based RAFT Agent. *Polym. Chem.* **2019**, *10*, 228–234. [CrossRef]
28. Lam, S.J.; O'BRien-Simpson, N.M.; Pantarat, N.; Sulistio, A.; Wong, E.H.H.; Chen, Y.-Y.; Lenzo, J.C.; Holden, J.A.; Blencowe, A.; Reynolds, E.C.; et al. Combating Multidrug-Resistant Gram-Negative Bacteria with Structurally Nanoengineered Antimicrobial Peptide Polymers. *Nat. Microbiol.* **2016**, *1*, 16162. [CrossRef]
29. Wong, E.H.; Khin, M.M.; Ravikumar, V.; Si, Z.; Rice, S.A.; Chan-Park, M. Modulating Antimicrobial Activity and Mammalian Cell Biocompatibility with Glucosamine-Functionalized Star Polymers. *Biomacromolecules* **2016**, *17*, 1170–1178. [CrossRef]
30. Bates, C.M.; Maher, M.J.; Janes, D.W.; Ellison, C.J.; Willson, C.G. Block Copolymer Lithography. *Macromolecules* **2014**, *47*, 2–12. [CrossRef]
31. Bates, M.W.; Barbon, S.M.; Levi, A.E.; Lewis, R.M.; Beech, H.K.; Vonk, K.M.; Zhang, C.; Fredrickson, G.H.; Hawker, C.J.; Bates, C.M. Synthesis and Self-Assembly of ABn Miktoarm Star Polymers. *ACS Macro Lett.* **2020**, *9*, 396–403. [CrossRef]
32. Levi, A.E.; Fu, L.; Lequieu, J.; Horne, J.D.; Blankenship, J.; Mukherjee, S.; Zhang, T.; Fredrickson, G.H.; Gutekunst, W.R.; Bates, C.M. Efficient Synthesis of Asymmetric Miktoarm Star Polymers. *Macromolecules* **2020**, *53*, 702–710. [CrossRef]
33. Workineh, Z.G.; Pellicane, G.; Tsige, M. Tuning Solvent Quality Induces Morphological Phase Transitions in Miktoarm Star Polymer Films. *Macromolecules* **2020**, *53*, 6151–6162. [CrossRef]
34. Rubinstein, M.; Colby, R.H. *Polymer Physics*; Oxford University Press: Oxford, UK, 2003.
35. Flory, P.J. *Principles of Polymer Chemistry*; Cornell University Press: New York, NY, USA, 1953.
36. Danel, Z.; Halun, J.; Karbowniczek, P. Analytical and numerical investigation of star polymers in confined geometries. *Int. J. Mol. Sci.* **2024**, *25*, 9561. [CrossRef] [PubMed]
37. Kremer, K.; Grest, G.S. Dynamics of entangled linear melts: A molecular-dynamics simulation. *J. Chem. Phys.* **1990**, *92*, 5057. Erratum in *J. Chem. Phys.* **1991**, *94*, 4103. [CrossRef]
38. Weeks, J.D.; Chandler, D.; Andersen, H.C. Role of repulsive forces in determining the equilibrium structure of simple liquids. *J. Chem. Phys.* **1971**, *54*, 5237. [CrossRef]

39. Lennard–Jones, J.E. Cohesion. *Proc. Phys. Soc.* **1931**, *43*, 461. [CrossRef]
40. Abraham, F.F.; Singh, Y. The structure of a hard sphere fluid in contact with a soft repulsive wall. *J. Chem. Phys.* **1977**, *67*, 2384. [CrossRef]
41. Lorentz, H.A. Ueber die Anwendung des Satzes vom Virial in der kinetischen Theorie der Gase Annalen der Physik. *Ann. Phys. Lpz.* **1881**, *248*, 127. [CrossRef]
42. Berthelot, D. Sur le melange des gaz. *C. R. Acad. Sci. Paris* **1898**, *126*, 1703.
43. Li, Y.-Y.; Zhang, X.-Z.; Cheng, H.; Kim, G.-C.; Cheng, S.-X.; Zhuo, R.-X. Novel stimuli-responsive micelle self-assembled from Y-shaped P(UA-Y-NIPAAm) copolymer for drug delivery. *Biomacromolecules* **2006**, *7*, 2956–2960. [CrossRef]
44. Zhang, H.-H.; Huang, Z.; Sun, B.; Guo, J.; Wang, J.; Chen, Y. Y-shaped poly(ethylene glycol) and poly(trimethylene carbonate) amphiphilic copolymer: Synthesis and for drug delivery. *J. Polym. Sci. Part A Polym. Chem.* **2008**, *46*, 8131–8140. [CrossRef]
45. Sonawane, S. J.; Kalhapure, R.S.; Jadhav, M.; Rambharose, S.; Mocktar, C.; Govender, T. AB_2-type amphipholic block copolymer containing a pH-cleavable hydrazone linkage for targeted antibiotic delivery. *Int. J. Pharm.* **2020**, *575*, 118948. [CrossRef] [PubMed]
46. Aghajanzadeh, M.; Andalib, S.; Danafar, H.; Rostamizadeh, K.; Sharafi, A. The effect of baicalein-loaded Y-shaped miktoarm copolymer on spatial memory and hippocampal expression of DHCR24, SELADIN and SIRT6 genes in rat model of Alzheimer. *Int. J. Pharm.* **2020**, *586*, 119546. [CrossRef]
47. Halun, J.; Karbowniczek, P.; Kuterba, P.; Danel, Z. Investigation of ring and star polymers in confined geometries:theory and simulations. *Entropy* **2021**, *23*, 242. Correction in *Entropy* **2022**, *24*, 413. [CrossRef]